JOTCS B
Journal of the Turkish Chemical Society
Section: B
Chemical Engineering
TURKISH CHEMICAL SOCIETY

Equilibrium and Kinetic of Ultrasound-Assisted Adsorption of Chromium (VI) ion from Electroplating Wastewater Using Melon Seed Husk Activated carbon

Esther BERNARD[1] and Adulfatai JIMOH[1]

Department of Chemical Engineering, School of infrastructure, Process and Engineering Technology Federal University of Technology Minna, PMB 65, Niger State, Nigeria.

Abstract: This study was focused on the removal of Cr(VI) ions from electroplating wastewater by ultrasound-assisted adsorption onto activated carbon obtained from melon seed husk. The activated carbon was produced by carbonization of crushed melon seed husk at a temperature of 500 °C for 15 min and further activation using 1.0 M concentration of potassium chloride (KCl) at a temperature of 500 °C for 90 min in a muffle furnace. The obtained adsorption isotherm data were better fitted to the Langmuir model than Freundlich model for adsorption both in the presence and absence of ultrasound (US). The adsorbent maximum adsorption capacity for Cr(VI) ion obtained from the Langmuir isotherms, were 5.059 mg/g and 2.031 mg/g both in the presence of ultrasound and its absence, respectively. The adsorption process in the presence and absence of ultrasound obeyed the pseudo-second-order kinetics. The SEM image of activated carbon before adsorption of metal ion revealed that the surface of activated carbon contains pores with different sizes and shapes, and also showed a significant change on the surface of activated carbon after interaction with Cr(VI) ions.

Keywords: Carbonization, activated carbon, melon seed husk, ultrasound-assisted adsorption.

Submitted: November 03, 2020. **Accepted:** November 11, 2021.

Cite this: Bernard E, Jimoh A. Equilibrium and Kinetic of Ultrasound-Assisted Adsorption of Chromium (VI) ion from Electroplating Wastewater Using Melon Seed Husk Activated carbon. JOTCSB. 2021;4(2):35–46.

***Corresponding author. E-mail:** estherbernard667@gmail.com.

INTRODUCTION

Currently, water contamination is a worldwide issue, with heavy metals contamination causing one of the most significant problems (1). Heavy metals are non-degradable, they are persistent, and accumulative in nature; hence they are carcinogenic agents that cause a serious threat to the living population (2). Nonetheless, certain heavy metals in little amounts are fundamental for a healthy life, yet enormous amounts and prolonged contact with these heavy metals may cause chronic toxicity. The toxicity caused by heavy metals includes reduced mental and central nervous function, gastrointestinal disorders, paralysis, ataxia, stomatitis, lowered energy level, damaging of the liver, lungs and other essential organs (3). Heavy metals are present practically in every region of present-day commercialization, from medicines to processed foods, construction materials to cosmetics; appliances to personal care products. It is very hard to avoid exposure to any of the many harmful heavy metals that are widespread in our environment (3). Among these metals, lead, nickel, cadmium, platinum, copper, lead, chromium, mercury, arsenic and antimony are of foremost concern (4). The effective recapture of heavy metals from wastewater and industrial wastewater before being disposed into the environment is of exceptional concern to researchers and engineers because of their unsafe impacts on humans and numerous living things. Thus, primary importance has been devoted to the need for the treatment of industrial wastewater effluent and as such both local and international authorities have established policies that made it mandatory for industrial wastewater to be treated to meet a set standard before been discharged into aqueous bodies (Table 1). To achieve such set standards, numerous methods have been employed for the treatment of

water contaminated with heavy metals. These methods include membrane processes, chemical precipitation, solvent extraction, electrochemical reduction, ion exchange, lime softening, coagulation/flocculation, and chitosan graphene oxide nanocomposites. Nevertheless, most of these mention treatment methods have limitations which include bulk poisonous sludge generation in flocculation/coagulation methods, renewal requirements during ion exchange, high operation cost, and large amounts of chemicals required using the chemical precipitation method (4).

However, the search for new methods that are sustainable in terms of efficiency, economy, energy, and environmentally friendly for the treatments of heavy metals in wastewater has attracted attention to the adsorption techniques (5).

Table 1: Permissible limits of heavy metals in drinking and wastewater by international institutes.

Heavy metals	**Permitted limits WHO*/EPA** (mg L^{-1})**	**References**
Zinc	5	(4)
Copper	1.0-1.5	(6)
Lead	0.005-0.015	(7)
Chromium	0.05-0.25	(4)
Arsenic	0.01	(4)
Mercury	0.002	(4)
Cadmium	0.005	(4)
Beryllium	0.004	(4)
Nickel	0.1	(7)

The use of activated carbon (AC) employed as adsorbent for the adsorption process has gained enormous attention due to its high internal surface area, small particle sizes, and active free valences. However, it might not be employed as an adsorbent for large-scale water treatment as a result of its high cost of production (4).

In recent times, low-cost and abundantly available natural materials such as agricultural waste materials have been employed as adsorbents and used to produce activated carbon for the removal of heavy metals in wastewater. These studies include rice husk, coir pith, orange peel, sawdust, peat, soybean, pine bark, banana peel and pith, rice bran cottonseed hulls, hazelnut shells, wool fibers, coconut shell, and saffron corn (8). Previous research has also shown that melon seed husk (*Citrullus colocynthis* L) is readily available and a good adsorbent for the removal of heavy metals. Melon belongs to the class of cucurbitaceae family, they are well-known to contain high oil and protein contents. It contains up to 35 % protein and 50 % oil, which is responsible for its wide cultivation and consumption worldwide (9). Melon seed husk has been used from adsorption studies of malachite green (10), Ni(II), Cr(III) and Co(II) (11) as well as Pb(II) and Cd(II) (12).

Although activated carbon has proven to be a suitable adsorbent, however, the relatively low adsorption rate of activated carbon due to its microporous and long diffusion pathway has necessitated the need for possible enhancement using ultrasonic irradiation. Ultrasound irradiation has been confirmed to accelerate the mass transfer process as a result of the phenomenon known as acoustic cavitation (13). Cavitation is the formation, growth, and consequent collapse of bubbles over a short time frame resulting in the generation of large degrees of energy over a specific location. Acoustic cavitation is the sound wave between the range of 16-100 kHz that produce pressure vibrations to generate the essential cavitation intensity (14). The employment of ultrasonic cavitation technology for wastewater treatment has been reported by researchers, although not yet been fully exploited (14). Raya and Zaria reported the use of rice husk activated carbon irradiated with ultrasound for the removal of Pb(II) in aqueous wastewater. The irradiated activated carbon adsorption capacity improved to 16.67 mg/g as against 9.80 mg/g when there was no irradiation and the process was described by the Langmuir isotherm model. Their findings showed that activated carbon adsorption capacity irradiated with ultrasonic waves was almost twice as much as the capacity of activated carbon adsorption without irradiation (15). Entezari and Soltani, reported the use of saffron corm irradiated with ultrasound for removal of Pb(II) and Cu(II) from binary aqueous solution, the obtained result indicates that the removal of both metal ions was greater in the presence of ultrasound than in absence of ultrasound (16). Furthermore, Schueller and Yang in their work found out that ultrasound acted as a mixer, which improved the mass transfer coefficients by means of cavitation and acoustic streaming (16). Since adsorption process is an easy

technique for the removal of pollutants from water and wastewater and the use of a cheaply available adsorbent which poses a high capacity for the removal of pollutants is very essential. Likewise, since the diffusion of species has a significant role in the adsorption process. Thus, the blending of the two referenced points was considered in this investigation. Activated carbon produced from melon seed husks was used as an adsorbent for the removal of Cr(VI) from electroplating wastewater in the presence and absence of ultrasound.

The mean purpose of this study is the use of ultrasound to aid adsorption of Cr(VI) ions from industrial wastewater (electroplating wastewater) onto activated carbon prepared from melon seed husks. The cavitation effects generated during ultra-sonication, creates shear stress that break up the activated surface and permits penetration of metal ions into the pores, also a localized turbulence of the solid-liquid film, during ultra-sonication accelerates the rate of mass transfer through the film by increasing the intrinsic mass transfer coefficient further pushes the adsorbates into the micropores. This increases pore division coefficient and increase the rate of adsorption.

Several research works has been carried out in the past, using activated carbon derived from agricultural waste products as adsorbent for the removal of different metal ions from simulated wastewater (aqueous wastewater) in absence of ultrasound. Although few works have been carried out on adsorption of metal ions from aqueous wastewater in presence of ultrasound (aided by ultrasound), none has been carried out with industrial wastewater (electroplating wastewater) in the presence of ultrasound. Table 2 shows previous works of the adsorption capacities (calculated from the Langmuir isotherm model) of activated carbon (obtained from agricultural waste products) of metal ions from aqueous wastewater.

Table 2: Activated carbon from Agricultural waste.

Agricultural waste	Adsorptive	$q_{m\ (mg;g)}$	Reference
Cob of the corn	Cu(II)	5.84–7.89	(17)
Melon seed husk	Ni(II)	-12.75	(11)
Melon seed husk	Co(II)	-38.39	(11)
Activated Carbon from Rice Husk,	Pb(II)	16.67[a]	(17)
		9.80[b]	
Hazelnut shell activate carbon	Cu(II)	3.05[a]	(17)
		3.77[b]	
Cob of the corn	Mn(VI)	0.53	(18)
Maple sawdust	Cd(II)	3.19	(19)
Bamboo-based Activated Charcoal	Pb(II)	4.792	(19)
Bamboo-based Activated Charcoal	Cd(II)	4.594	(19)
Bamboo dust	Pb(II)	4.771	(19)
Bamboo dust	Cd(II)	4.400	(19)

[a] in the presence of US
[b] in the absence of US

MATERIALS AND METHODS

Materials

Melon seed husk sample was obtained from Mina, Niger State, Nigeria. The husk was washed thoroughly with distilled water to remove foreign materials present on the surface. The washed sample was further oven-dried at a temperature of 100 °C and crushed with a mechanical crusher to reduce the size. The crushed samples were carbonized at a temperature of 500 °C for 15 min. 25 g of the carbonized sample was mixed in 50 mL of 1.0 M concentration of potassium chloride and allowed to soak for 24 h at room temperature. It was later oven-dried for 30 min at 100 °C. The dried carbonized samples were further transferred into a muffle furnace and activated at a temperature of 500 °C for 90 min. The obtained activated carbon was then transferred into a desiccator to cool. Thereafter the sample was carefully rinsed using 0.1 M of HCl and distilled water to eliminate the residual salt present until the pH of filtrate reached 7.

Batch Adsorption Experiment

Set-up

Adsorption study was carried out using an ultrasonic cleaning bath, with model number SB25-12DT, operating at 40 kHz and equipped with a temperature regulator. Distilled water was added to the cleaning bath up to one third (1/3) of the volume of the cleaning bath. 0.6 g of activated carbon was added into 50 mL of electroplating wastewater of known concentration and pH which was kept in 250 mL Erlenmeyer flasks, which were placed into the carrier fitted in the ultrasonic bath. A temperature of 30 °C was maintained during ultrasonic irradiation by water circulating from a thermostatic bath utilizing a pump. The suspensions were sonicated for a given period time and the operating frequency was maintained at 40 kHz.

Adsorption studies were also carried out in the absence of ultrasound (conventional method) using a water-bath shaker with an operating speed of 200 rpm and at 30 °C.

Equilibrium experiments
The industrial wastewater used was collected from the electroplating section of the Scientific Equipment Development Institute (SEDI), Niger State. The wastewater contained Cr(VI) ions. The initial concentration of Cr(VI) found in the wastewater sample was 18.28 ppm. The initial pH of the wastewater was 3.5 and was adjusted to pH 4 for adsorption studies using 0.1 N NaOH.

The equilibrium adsorption experiment was conducted in 250 mL Erlenmeyer flasks containing 0.6 g of adsorbent with 50 mL of electroplating wastewater which was sonicated for 90 min in an ultrasonic cleaning bath until equilibrium was reached. Adsorption studies using the conventional method were also carried out in 250 mL Erlenmeyer flasks containing 0.6 g of adsorbent with 50 mL of electroplating wastewater. The flasks were agitated for 90 min at 200 rpm. After the sonication and agitation, the supernatant was centrifuged and analyzed using an atomic absorption spectrophotometer for residual metal ions concentration.

The amount of Cr(VI) ions adsorbed at any given time was calculated using equation (1).

$$q=\frac{(C_0-C)V}{M} \quad (1)$$

Where q is the number of metal ions (Cr(VI) ions) adsorbed at time t, C_0 and C are the initial metal ions concentrations and metal ions concentrations at time t respectively. V is the volume of wastewater used (50 mL) and M is the amount of adsorbent in industrial wastewater (0.6 g) used.

RESULTS AND DISCUSSION

Characterization of Activated Carbon

The prepared activated carbon from melon seed husk by a two-step process of carbonization at 500 °C for 15 minutes and then activation with KCl at 500 °C for 90 min was characterized by standard methods (Table 3). The obtained specific surface area by BET analysis was 1285.75 m^2/g and the obtained iodine number of 1251 mg/g are the highest so far reported for activated carbon obtained from the melon husk. Formaldehyde and sodium hydroxide (20) impregnated activated carbons from melon husk had a specific surface area of 395 and 1187 m^2/g respectively. Therefore, the prolonged impregnation with KCl and the two-step activation process adopted favored the formation of porous activated carbon.

Table 3: The properties of activated carbon prepared from melon seed husk.

Characteristic	Method	Value
Specific surface area	BET, N_2	1285.751 m^2/g
Iodine value	ASTM D 4607	1251 mg/g
Ash	ASTMD2866	9.0
Total Pore volume	ASTMD 4607	0.47 cm^3/g
Pore size		3.191 cm^3/g

Adsorption Isotherms
The adsorption of Cr(VI) from electroplating wastewater on activated carbon from the melon husk (AC) was conducted in the presence and absence of ultrasound (US) at 30 °C. As shown in Figure 1, the amount of Cr(VI) adsorbed on AC in the presence of the US is greater than the amount in absence of the US. The increased amount of adsorbed Cr(VI) on AC in presence of the US is a result of acoustic cavitation which is the formation, growth, and violent collapse of cavitation bubbles. Also, the shear forces generated during the cavitation are typically mostly responsible for the enhanced removal of the metal ions in the presence of the US (17).

To investigate and further describe adsorption, isotherm models were employed. The most frequent models used are the Langmuir and Freundlich isotherms (Table 4). In this current work, the relationships between the amount of Cr(VI) adsorbed and its equilibrium concentration in wastewater in the presence and absence of US for 90 min at 30 °C were modeled by both Langmuir and Freundlich isotherm models. The Langmuir model is used to describe the homogeneous sorption, in which each sorption molecule has equal sorption energy as the other, while the Freundlich isotherm is used to describe sorption characteristics for the heterogeneous surface. Langmuir constants a_L and q_m and Freundlich constants K_F and b_F are presented in Table 5. The ratio of adsorption and desorption is defined by Langmuir adsorption constant a_L and it is also related to the free energy of adsorption.

Figures 2 and 3 showed that the two isotherms models employed both in the presence of the US and in its absence were well fitted by both models used as a result of the good fits attained (R^2 close to

1). However better fitting was provided by the Langmuir model.

The value of a_L represents the affinity of Cr(VI) to the adsorbent. The value of a_L for US-adsorption was higher when compared to adsorption in absence of US as evident in Table 5, which implies that the introduction of US positively affected the affinity of Cr(VI) on AC. Identical findings were obtained by Milenković *et al.* (8) for the adsorption of Cu(II) ions on hazelnut activated carbon in the presence of US at a frequency of 40 kHz. A similar observation was drawn from values of Freundlich constant K_F, which has a higher value in the presence of the US than its value in the absence of US adsorption.

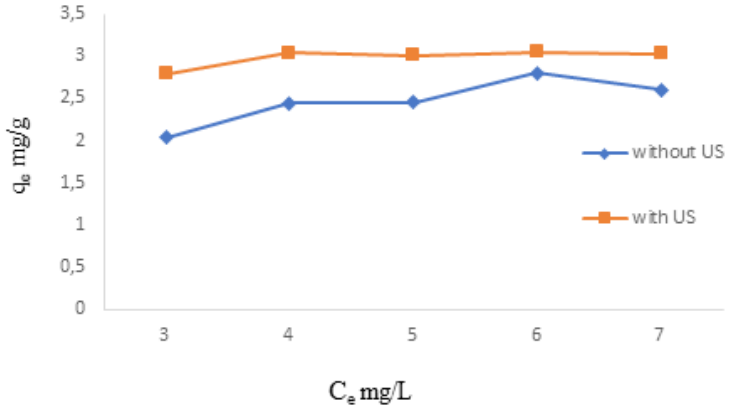

Figure 1: Adsorption isotherms of Cr(VI) ions on AC from melon seed husks in the absence (♦) and the presence (■) of ultrasound at 30 °C.

Table 4: Adsorption isotherms.

Isotherm	Integral form	Linear form
Langmuir	$q_e = \frac{k_L C_e}{1 + a_L C_e}$	$\frac{C_e}{q_e} = \frac{1}{k_L} + \frac{a_L}{k_L} \times C_e$
Freundlich	$q_e = K_F C_e^{b_F}$	$\ln q_e = \ln K_F + b_F \ln C_e$

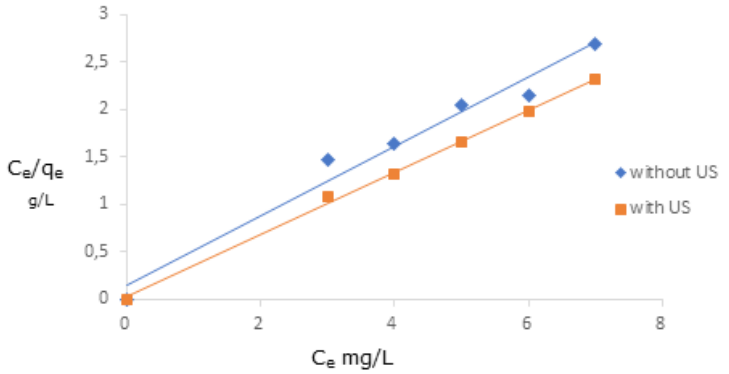

Figure 2: Linear forms of the Langmuir model adsorption isotherms of Cr(VI) ions on AC from melon seed husks in the absence (♦) and the presence (■) of ultrasound at 30 °C.

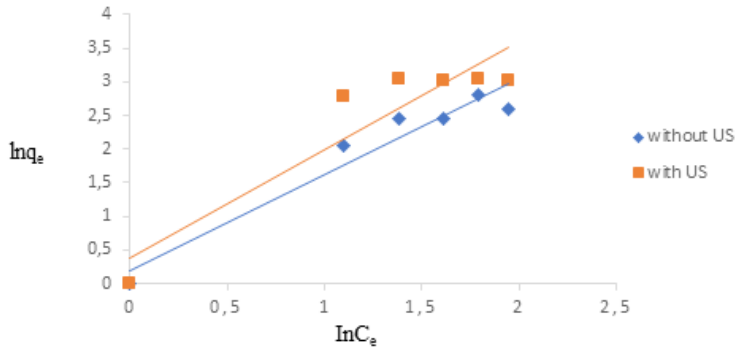

Figure 3: Linear forms of the Freundlich adsorption isotherms of Cr(VI) ions on AC from melon seed husks in the absence (♦) and the presence (■) of ultrasound at 30 °C.

Table 5: Adsorption isotherms parameters, linear correlation coefficient, and standard deviation.

Isotherm	**Parameter**	**Silent adsorption**	**Ultrasound-assisted adsorption**
Langmuir	a_L (L/mg)	2.591	11.802
	q_m (mg/g)	2.031	5.059
	R	0.998	0.972
Freundlich	b_F	1.425	1.606
	K_F	1.218	1.474
	R	0.939	0.863

It was also observed from Table 5 that the monolayer saturation capacity at equilibrium q_m in the presence of US was larger than that in the absence of US adsorption (2.031 mg/g and 5.059 mg/g respectively), which could be ascribed to cavity effects that aid the adsorption process.

Figure 4 shows the amount of Cr(VI) ions adsorbed on AC obtained from melon seed husk both in the presence of US and adsorption in the absence of US at 30 °C. The adsorption study was carried out up to a contact time of 135 min to obtain equilibrium time. At the start of the adsorption process Cr(VI) ions were swiftly adsorbed, but which later slowed down, until equilibrium was finally reached. The highest rate of Cr(VI) ion removal at the start of adsorption was perhaps due to the available large surface area on the adsorbent existing for adsorption and the strong interaction amongst the Cr(VI) ions and the surface of the adsorbent. At the later stage of the adsorption process, the surface adsorption sites became exhausted and the rate of removal was controlled by the rate of Cr(VI) ion transportation from the external to the internal sites of the adsorbent particles. In the presence of ultrasound, the removal of Cr(VI) was higher than in the absence of ultrasound and this could be attributed to the result of the cavitation process which enhances the diffusion process.

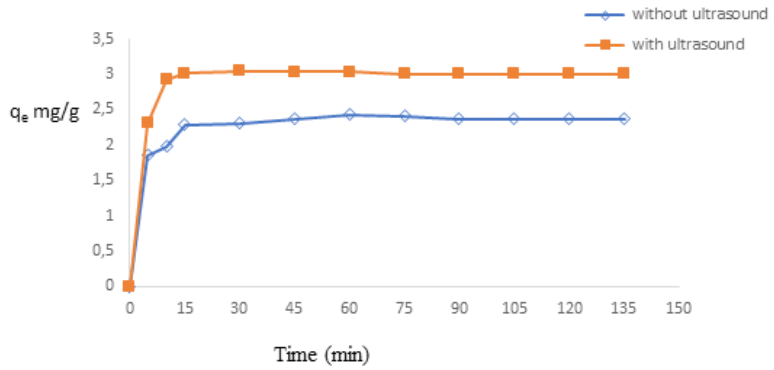

Figure 4: Adsorption of Cr(VI) ions on AC from melon seed husk in the absence ( ) and the presence ( ) of ultrasound at 30 °C.

Adsorption kinetics mechanism

Three kinetic models namely the pseudo-first-order, pseudo-second-order and intraparticle diffusion were employed to study the controlling mechanism of the adsorption process of Cr(VI) ions on the adsorbent in this current study. Several steps are involved in the liquid-solid adsorption process, which includes the diffusion of the solute from the solution to the film surrounding the sorbent particles, the solute diffusion from the particle surface through the pores into the internal active sites, and the adsorption of solute from active sites by various mechanisms. The entire sorption rate is controlled by the rate of each step. The differential, integral, and linear forms of the kinetic models are shown in Table 5. The values of the kinetic model parameters used and the linear forms of the linear correlation coefficient are shown in Table 6. When the pseudo-second-order kinetics was applied, the values of equilibrium amount of Cr(VI) ions adsorbed qe, was obtained from the non-linear regression, and considering that the exponential growth of the amount of Cr(VI) ions adsorbed with time (qe =2.999 and 2.489 mg/g for adsorption in presence of ultrasound and absence of ultrasound respectively).

From the plot of the linear forms of the three kinetic model curves shown in Figure 5, it was observed that only the pseudo-second-order kinetic model applied fitted well with the experimental data, which has a linear correlation coefficient of 1. The pseudo-second-order kinetic model shown in Figure 6 has the best fit to the experimental data for both adsorptions in the presence of ultrasound and adsorption in the absence of ultrasound. The pseudo- second-order kinetic model assumes that rate-limiting steps could be a result of a chemical reactions between adsorbent and adsorbate. Therefore, the pseudo-second-order kinetic model is possibly the generalized kinetic model for the adsorption system studied. Milenković et al (8) reported related findings of the applicability of a similar kinetic model and the second-order nature of adsorption of Cu(II) ions on activated carbon gotten from hazelnut shells.

Table 6: Kinetic Models.

Kinetic Model	Differential form	Integral form	Linear form
Pseudo-first order	$\frac{dq}{dt}=k_1(q_e-q)$	$q=q_e(1-e^{-k_1 t})$	$\ln\left(\frac{q_e-q}{q_e}\right)=-k_1 t$
Pseudo-second order	$\frac{dq}{qt}=k_2(q_e-q)^2$	$q=\frac{k_2 q_e^2 t}{1+k_2 q_e t}$	$\frac{t}{q}=\frac{1}{k_2 q_e^2}+\frac{1}{q_e}t$
Intra-particle diffusion	$\frac{\partial q}{\partial t}=D_{eff}\frac{\partial^2 q}{\partial t^2}$	$q=k_p\sqrt{t}+C_1$	$q=k_p\sqrt{t}+C_1$

Table 7: Parameters of kinetic models and linear correlation coefficient deviation.

Kinetic Model	Model Parameters	Silent Adsorption	Ultrasound-assisted adsorption
Pseudo-first order	k_1(min^{-1})	0.009	0.004
	R	0.513	0.142
Pseudo-second order			
	K_2(g/mg min)	1.178	9.756
	q_e	2.489	2.999
	R	0.999	1.000

Intraparticle diffusion			
First Stage	Kp (mg/g $min^{0.5}$)	0.129	0.152
	C_1 (mg/g)	1.231	1.683
	R	0.501	0.422

In the present study, of the three kinetic models employed, the pseudo-second-order model gave the best fit of experimental data and has the highest linear correlation coefficient of R = 1 and R= 0.999 for adsorption in presence of US and absence of US respectively. The Pseudo-second-order model is founded on the assumption that the rate-limiting step may well be a chemical reaction between the adsorbent and the adsorbate. Thus, for the adsorption system studied, the possibly generalized kinetic model is the pseudo-second-order kinetic. Babarinde et al (11) reported the applicability of a similar kinetic model and the second-order nature of the adsorption process of Cr(VI) ion on melon seed husk as adsorbent. The rate constant for the reaction of pseudo-second-order was positively affected the US in the present study, its values being K_2 = 9.756 g/mg min and K_2 = 1.178 g/mg min in the presence and absence of US, respectively. The intra- particle diffusion model was also employed to identify the diffusion mechanism because both the pseudo-first-order model and the pseudo-second-order model could not identify it.

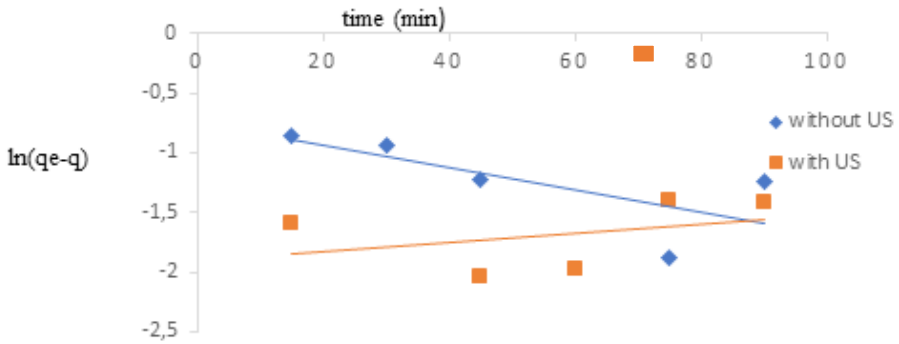

Figure 5: Pseudo-first-order kinetic model for the removal of Cr(VI) ions on AC from melon seed husk in the absence ( ) and the presence ( ) of ultrasound at 30 °C.

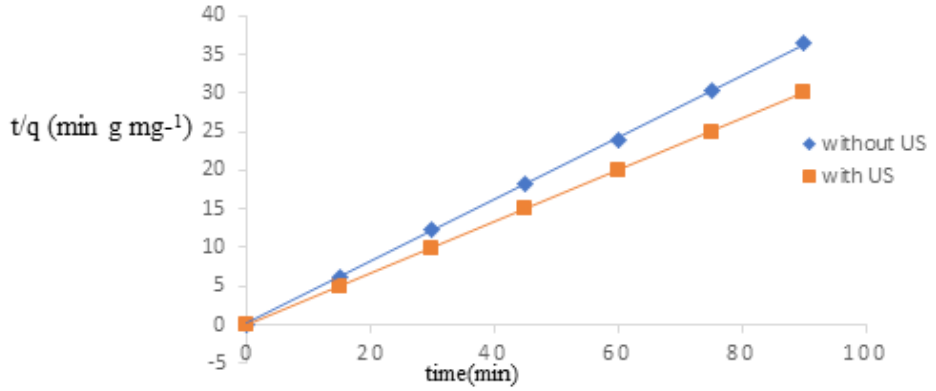

Figure 6: Pseudo-second-order kinetic model for the removal of Cr(VI) ions on AC from melon seed husk in the absence ( ) and the presence ( ) of ultrasound at 30 °C.

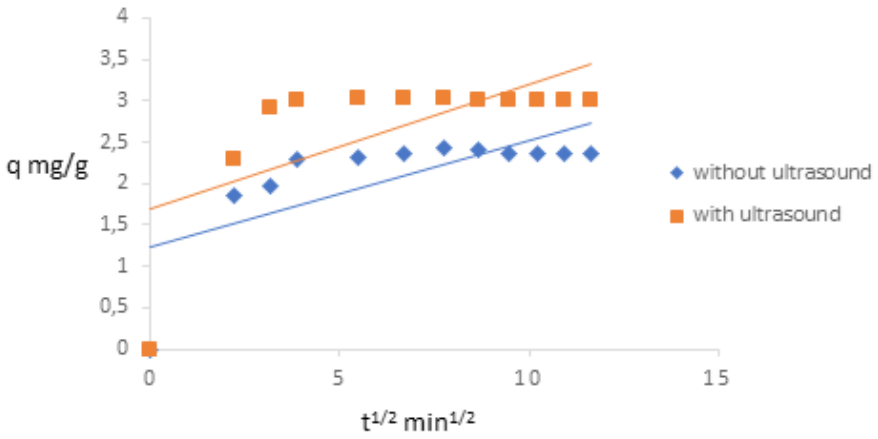

Figure 7: Intra particle diffusion model for the removal of Cr(VI) ions on AC from melon seed husk in the absence (♦) and the presence (■) of ultrasound at 30 °C.

Figure 7 shows the plot of q verse $t^{1/2}$ both in the presence and absence of US. Intraparticle diffusion is the sole rate determining step if the plot of qt versus $t^{1/2}$ is linear and passes through the origin (C =0). In the adsorption process, the plot did not pass through the origin, which specifies the existence of some boundary layer effect and disclosed that intraparticle diffusion is not the rate determining step in overall sorption process.

When comparing the adsorption in absence of ultrasound (silent adsorption) to that in presence of ultrasound, the intra-particle diffusion rates in the presence of US has increased approximately by 18% compared to adsorption in absence of US. The intercept value C_1 for both adsorptions in presence of US and absence of US is given in Table 6. The greater intercept value (C_1) in presence of the US depicts higher ultrasound-assisted adsorption of activated carbon from the melon seed husk, compared to adsorption in absence of ultrasound (21).

The SEM image of AC before adsorption of metal ions shown in Figure 8 (a), revealed that the surface of AC contains pores with different sizes and shapes, while Figure 8 (b), revealed that there were significant changes on the surface of AC after interaction with Cr(VI) ions. Some of the pores before adsorption have been closed after interaction with Cr(VI) ions and flake like deposits were also observed on the surface of AC after adsorption.

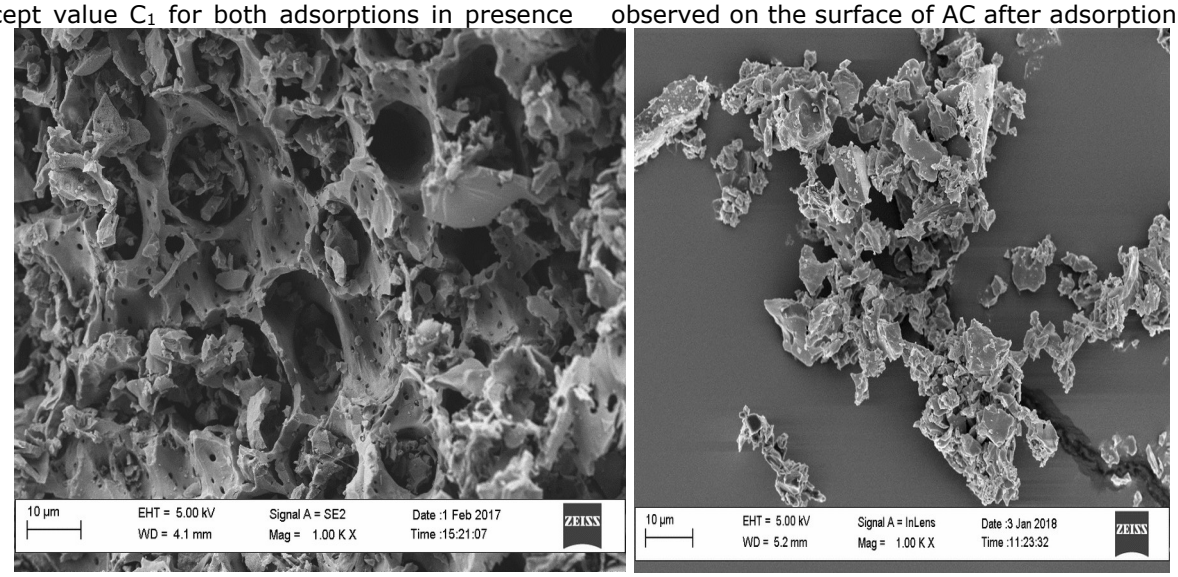

Figure 8: SEM images of AC (left) before and after (right) adsorption at 1,000 magnification.

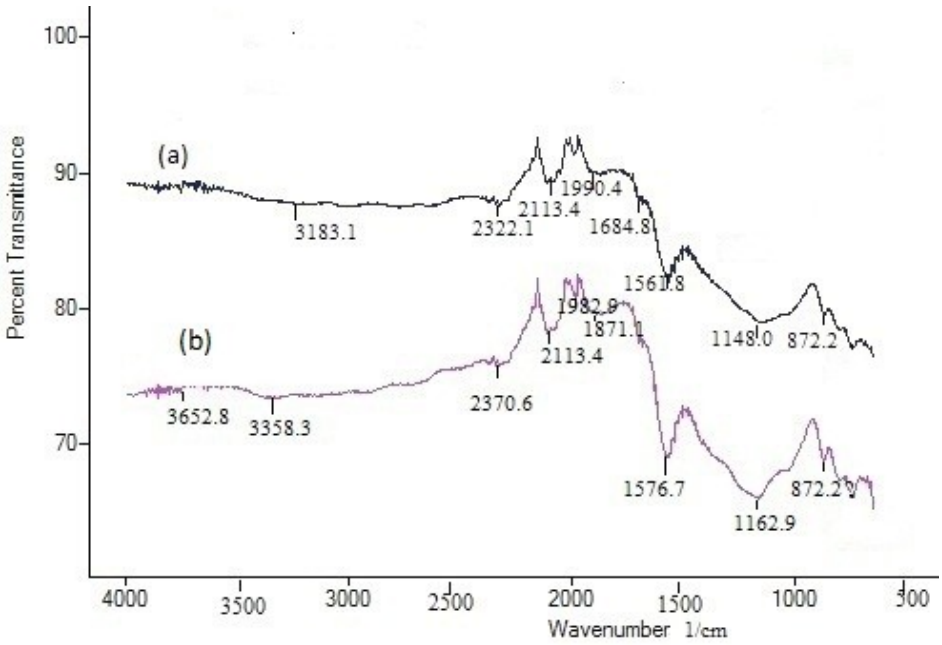

Figure 9: FTIR analysis of activated carbon from melon husk (ACM) and ACM after adsorption.

The FTIR spectrum of the activated carbon from melon husk was carried out to reveal the active surface functional groups, responsible for binding of Cr(VI) ion. The FTIR spectra (a) of activated carbon showed O–H stretching band, of decreased intensity, appeared at 3183.1 cm^{-1}, due to cleaving of phenolic groups during activation, the O–H stretching band at 3183.1 cm^{-1} present on the FTIR spectra of activated carbon (a) was shifted to 3358.3 on the FTIR spectra (b) of activated carbon loaded with Cr(VI) ions with appearance of a new band at 3652.8 cm^{-1} after adsorption. Similarly, the peaks at 2322.1, 1561.8 and 1148.0 cm^{-1} present on the FTIR spectra (a) of activated carbon (were shifted to 2370.6, 1576.7 and 1162.9 cm^{-1} on the FTIR spectra (b) of activated carbon respectively after adsorption, the shift in positions was as a result of attachment of the Cr(VI) ions to the activated carbon through these functional groups. While the peak at 1684.8 cm^{-1} present on the FTIR spectra (a) of activated carbon disappeared after adsorption of Cr(VI) ions as evident in spectra (b). The disappearance of peak suggest that there was chemical interactions between the adsorbed Cr(VI) ions and functional groups. The result is consistent with the works of Giwa *et al* (2013) of which the FTIR spectra of the activated carbon obtained from melon husk had a shift in the position of the functional group of C=O and –NH at 1624 cm^{-1} and 3454 cm^{-1}, were shifted to 1629 $cm^{-1}$and 3448 cm^{-1} respectively after adsorption of cadmium ion.

CONCLUSION

A two-step process of carbonization and subsequently chemical activation was employed for the production of activated carbon from melon seed husk with a higher specific surface area compared to other activated carbons previously produced from melon seed husk. This implies that carbonization and subsequent chemical activation lead to activated carbon with well- developed pores. The average pore size suggested that the produced activated carbons are mainly mesoporous. The obtained adsorption isotherm data for removal of Cr(VI) ion from electroplating wastewater was well fitted to the Langmuir model than the Freundlich model for both adsorptions assisted by ultrasound and adsorption in absence of ultrasound. Higher R values were obtained from the Langmuir model, which could be possibly due to the homogeneous distribution of active sites on the activated carbon surfaces. Furthermore, the kinetics of Cr(VI) ion adsorption on the melon seed husk activated carbon follows the pseudo-second-order model, which indicates that chemisorption may be the rate-limiting step. The prime benefit of sonication based on the data obtained was a higher speed of adsorption, particularly during the initial period. In the presence of ultra-sonication, the rate constant of pseudo-second-order was increased by 88 % when compared to that in the absence of ultra-sonication. Activated carbon from melon seed husk is an effective adsorbent for removal of Cr(VI) ion from electroplating wastewater, even though the production process was relatively simple and from a cheap available waste product, the conclusion of the use of activated carbon obtained from melon seed husk for removal of Cr(VI) ion, other heavy metals and other pollutants should only be withdrawn when after only a thorough techno-economic analysis of the complete removal process. The SEM image showed a significant change after the adsorption of Cr(VI) ions.

REFERENCES

1. Alghamdi AA, Al-Odayni A-B, Saeed WS, Al-Kahtani A, Alharthi FA, Aouak T. Efficient Adsorption of Lead (II) from Aqueous Phase Solutions Using Polypyrrole-Based Activated Carbon. Materials. 2019 Jun 24;12(12):2020. <DOI>.

2. Rao RAK, Kashifuddin M. Kinetics and isotherm studies of Cd(II) adsorption from aqueous solution utilizing seeds of bottlebrush plant (Callistemon chisholmii). Appl Water Sci. 2014 Dec;4(4):371–83. <DOI>.

3. Chaturvedi D, Sahu O. Adsorption of heavy metal ions from wastewater. Global Journal of Environmental Science and Technology. 2014;2(3):020–8.

4. Shafiq M, Alazba A, Amin M. Removal of heavy metals from wastewater using date palm as a biosorbent: a comparative review. Sains Malaysiana. 2018;47(1):35–49.

5. Kanawade SM, Gaikwad R. Removal of zinc ions from industrial effluent by using cork powder as adsorbent. International journal of chemical engineering and applications. 2011;2(3):199.

6. Bilal M, Shah JA, Ashfaq T, Gardazi SMH, Tahir AA, Pervez A, et al. Waste biomass adsorbents for copper removal from industrial wastewater—A review. Journal of Hazardous Materials. 2013 Dec;263:322–33. <DOI>.

7. Abdel-Raouf M, Abdul-Raheim A. Removal of heavy metals from industrial waste water by biomass-based materials: a review. J Pollut Effects Control. 2017;5(1):1–13.

8. Milenković DD, Dašić PV, Veljković VB. Ultrasound-assisted adsorption of copper(II) ions on hazelnut shell activated carbon. Ultrasonics Sonochemistry. 2009 Apr;16(4):557–63. <DOI>.

9. Giwa S, Abdullah LC, Adam NM. Investigating "Egusi" (Citrullus Colocynthis L.) Seed Oil as Potential Biodiesel Feedstock. Energies. 2010 Mar 30;3(4):607–18. <DOI>.

10. Idris S, Yisa J, Muhammed NM, Chioma C. Equilibrium and Adsorption Studies of Malachite Green onto Melon Seed Shell Activated Carbon. Int J Modern Chem. 2013;4(2):90–103.

11. Babarinde A, Omisore GO, Babalola JO. Kinetic, isothermal and thermodynamic parameters for the biosorption of Ni (II), Cr (III), and Co (II) onto Melon (Citrillus lanatus) seed husk. International Journal of Chemical and Biochemical Sciences. 2014;6:18–33.

12. Nwankwo D, Sylvanus Chima E, Tochukwu M. Comparative study of the Bioadsorbtion of Cadmium and lead from industrial waste water using melon (citrullus colocynthis) husk activated with sulphuric acid. American Journal of Environmental Protection. 2014;1(1):1–8.

13. Hamdaoui O, Naffrechoux E. Adsorption kinetics of 4-chlorophenol onto granular activated carbon in the presence of high frequency ultrasound. Ultrasonics Sonochemistry. 2009 Jan;16(1):15–22. <DOI>.

14. Parthasarathy S, Mohammed RR, Fong CM, Gomes RL, Manickam S. A novel hybrid approach of activated carbon and ultrasound cavitation for the intensification of palm oil mill effluent (POME) polishing. Journal of Cleaner Production. 2016 Jan;112:1218–26. <DOI>.

15. Raya I, Zakir M. The adsorption of Pb (II) ions on activated carbon from rice husk, irradiated by ultrasonic waves: kinetic and thermodynamics studies. Journal of Natural Sciences Research. 2014;4(2):18–24.

16. Entezari MH, Soltani T. Simultaneous removal of copper and lead ions from a binary solution by sono-sorption process. Journal of Hazardous Materials. 2008 Dec;160(1):88–93. <DOI>.

17. Milenković DD, Bojić ALj, Veljković VB. Ultrasound-assisted adsorption of 4-dodecylbenzene sulfonate from aqueous solutions by corn cob activated carbon. Ultrasonics Sonochemistry. 2013 May;20(3):955–62. <DOI>.

18. Norozi F, Haghdoost G. Application of corncob as a natural adsorbent for the removal of Mn (VII) ions from aqueous solutions. Orient J Chem. 2016;32(4):2263–8.

19. Odoemelam SA, Onwu FK, Uchechukwu SC, Chinedu MA. Adsorption isotherm studies of Cd (ll) and Pb (ll) ions from aqueous solutions by bamboo-based activated charcoal and bamboo dust. American Chemical Science Journal. 2015;5(3):253–69.

20. Foo KY, Hameed BH. Preparation and characterization of activated carbon from melon (Citrullus vulgaris) seed hull by microwave-induced NaOH activation. Desalination and Water Treatment. 2012 Sep;47(1–3):130–8. <DOI>.

21. Igwe JC, Abia A, Ibeh C. Adsorption kinetics and intraparticulate diffusivities of Hg, As and Pb ions on unmodified and thiolated coconut fiber. International Journal of Environmental Science & Technology. 2008;5(1):83–92.

NOMENCLATURE

US Ultrasound

AC activated carbon

K_1 rate constant of pseudo-first- order sorption (min^{-1})

K_2 rate constant of pseudo-first -order sorption (min^{-1})

K_L Langmuir equilibrium constant (L/mg)

K_F Freundlich constant((mg/g)/(mg/L)b_F)

a_L Langmuir constant (L/mg)

b_F Freundlich exponent (dimensionless)

Co initial metal ions concentration

C metal ions concentrations at time t

C_1 constant of the intra particular diffusion model (mg/g)

M amount of adsorbent in industrial wastewater (g)

q amount of metal ions adsorbed at time t,

qe amount of metal ions uptake at equilibrium per unit mass of adsorbent (mg/g)

q_{max} maximum monolayer adsorption capacity of the adsorbent (mg/g)

R coefficient of linear correlation

V volume of wastewater

t time (min)